A UAV Laser Scanning Technique for Automated Mapping of In-Stope Structural Discontinuity Sets in Underground Mines

Dibyayan Patra
School of Minerals and Energy Resources Engineering
University of New South Wales
Sydney, Australia
d.patra@unsw.edu.au

Charles Baylis
Broken Hill Propriety Company Ltd.
Carrapateena, Australia
charles.baylis@bhp.com

Pasindu Ranasinghe
School of Minerals and Energy Resources Engineering
University of New South Wales
Sydney, Australia
pasindu.ranasinghe@unsw.edu.au

Bikram Banerjee
School of Surveying and Built Environment
University of Southern Queensland
Toowoomba, Australia
bikram.banerjee@unisq.edu.au

Simit Raval
School of Minerals and Energy Resources Engineering
University of New South Wales
Sydney, Australia
simit@unsw.edu.au

***Abstract*—Underground mapping and identification of exposed rock mass structures or discontinuity sets is critical in challenging mine regions like stopes for stability analysis and plays a key role in terms of both the economic and safety aspects of an excavation site. However, utilisation of traditional mapping equipment is not feasible in a stope due to the challenges posed by limited accessibility, complex geometries of stopes, unavailability of global navigation satellite system (GNSS), and safety risks. Recent advances in unmanned aerial vehicles (UAV), portable mobile laser scanning (MLS) LiDAR technology, and simultaneous localization and mapping (SLAM) have led to the development of UAV laser scanners, allowing engineering personnel to remotely obtain 3D point clouds from such challenging regions. This study investigates the use of a UAV laser scanning system for acquiring 3D point cloud of an underground metal mining stope to perform automated mapping of discontinuity sets in the exposed stope surface.**

Keywords—stope mining, UAV laser scanning, structure mapping, discontinuity sets

I. Introduction

In underground metal mining operations, stopes are large excavated chambers that serve as fundamental elements designed to maximise ore recovery and economic efficiency. Mapping structural discontinuities in stopes is crucial for ensuring and maintaining safety, stability and efficiency during ore excavation. Discontinuities, such as joints, fractures, and faults, act as planes of weakness that can lead to sliding, wedge failures, or rockfalls, compromising stope walls and roofs [1, 2]. Mapping exposed rock mass structures and discontinuity sets enables geotechnical engineers to predict failure mechanisms, optimise stope design to minimise interactions with unfavourable structures, and reduce overbreak [3]. Additionally, discontinuity data can also enhance geotechnical models and kinematic analysis for stopes, aiding in stress analysis and stability assessments, ultimately ensuring safer and more cost-effective stope operations.

Traditional methods like terrestrial laser scanners (TLS) and slope stability radars (SSR) are widely dominant for structure mapping in surface mining, whereas handheld and vehicle-mounted SLAM-based mobile laser scanners (MLS) play a major role in underground mining tunnels [2]. However, such methods are not ideal for 3D point cloud data capture in complex underground regions like stopes due to several challenges such as inaccessibility, complex stope geometries, lack of GNSS, structural instabilities, poor lighting conditions and stringent safety requirements. To overcome these accessibility challenges, an optimal remote point cloud capture mechanism is required for structure mapping in underground stopes. Recent advances in UAV and portable SLAM-based MLS LiDARs have led to the development of UAV laser scanning systems [4-6] that can enable personnel to capture point clouds from inaccessible areas like stope without the need for a GNSS signal.

In this study, the use of a UAV laser scanning system to acquire 3D point clouds of underground metal mining stopes was explored to identify and map discontinuity sets in exposed surface structures of stopes using an automated structure mapping technique. Using an automated method instead of manual identification significantly reduces processing time as well as human biases.

II. Materials and Methods

This section details the technology and instrumentation used for the data collection, study area and data acquisition, and the adopted processing and structure mapping workflow.

A. Technology

The development of UAV laser scanning systems enables remote mapping of limited accessibility areas in underground

mines like stopes. In this study, the authors have used a Hovermap scanner [7], a SLAM-based MLS LiDAR system, coupled with a DJI Enterprise M210 Drone. The Hovermap UAV laser scanning system (Table 1) that has been utilized for this study includes:

- A fully integrated Hovermap scanner consisting of 16-channel Velodyne LiDAR (VLP-16) fixed on a mechanical 360º rotating head, inertial measurement unit (IMU) and an onboard computer. VLP-16 has a 360º horizontal field of view and a 30º vertical field of view, therefore rotating the sensor around its horizon produces a spherical field of view.
- The system integrates real-time scan data from the Hovermap into the UAV flight controller, thereby enabling autonomous position hold and collision avoidance in GNSS-denied underground environments.
- A SLAM package (Wildcat SLAM by CSIRO) for post-processing the raw data acquired by the IMU and laser scanner to produce a high-resolution 3D point cloud. The accurate co-registration of the LiDAR frames in GNSS-denied environments is achieved through the application of SLAM, leveraging a precise embedded IMU chip.

TABLE I. SPECIFICATIONS OF THE UAV LASER SCANNING SYSTEM

Hovermap UAV laser scanning system

Dimensions	887 x 880 x 378 mm
Weight	5.41 kg
Laser range	100 m
Range accuracy	± 3 cm
Angular resolution	0.4º horizontal 2º vertical
Scan rate	300,000 points/s
Sensors and accessories	Laser scanner, IMU, onboard computer, UAV, flight controller, data storage, batteries

B. *Study area and data acquisition*

The stope area used for this study is from an underground metal mine, Olympic Dam. Olympic Dam is located in South Australia (approximately 575 km northwest of the capital Adelaide). The mining operations occur about 900 m below sea level spanning a 3 km by 6 km area. At this site, large polymetallic orebodies are mined using a sub-level open stope mining method with the stopes blasted in two or more blast packets. The stopes range from single lift to multiple lifts with heights between 25 m to 200 m. Every stope is accessible from the bottom draw point and most from the top crown level, while larger stopes also have midlevel accesses.

For this study, the authors selected a stope placed between sub-levels 41 and 46 (Fig. 1). The height of the stope is approximately 50 m, and the width at the widest point is 28 m. The point cloud data from this stope has been collected in a single loop trajectory using the UAV laser scanning system. The flight speed was maintained around a nominal 1 m/s, considering a scan rate of 300,000 points/s, to produce a dense point cloud. A total of ~5 minutes was taken to complete the scan of the stope.

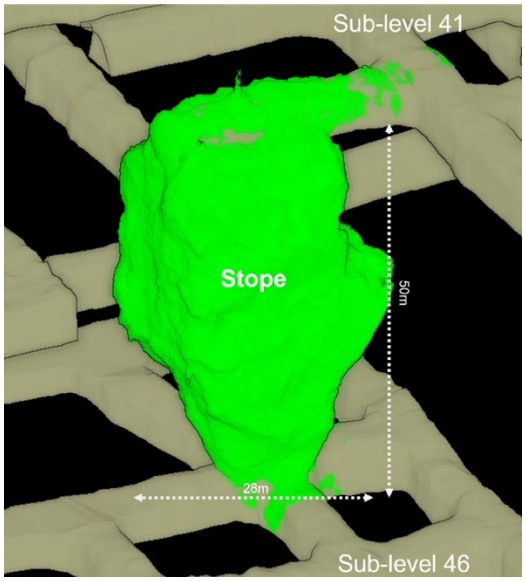

Fig. 1. Point cloud of selected stope in the study area

C. *Processing workflow for structure mapping*

The following processing steps were applied to the data collected by the UAV laser scanning system.

Pre-processing: The raw data collected by the Hovermap scanner is processed by the Wildcat SLAM package to produce a point cloud (.las) file. The point cloud is then georeferenced to align the local coordinate system to the mine's grid system. Finally, the resulting point cloud is downsampled using a grid downsampling method (with voxel size of 10 cm used for this study). This process ensures a uniform point density by eliminating redundant points caused by laser backscattering and noise, while also reducing the file size for faster processing.

Automated structure mapping: After the 3D point cloud is acquired from the stope and pre-processed, the next step is to identify and map the structural discontinuities inside the stope surface. For this, a structure mapping algorithm Discontinuity Set Extractor (DSE) has been used [8]. Following are the steps of the technique:

- First, the normal vector is computed for each point in the point cloud using k-nearest neighbours method, with k set to 30 in this study.
- A plane is fitted to the selected neighbours, and the normal vector is derived from this plane.
- Using the computed normal vectors, the orientation (dip angle DA and dip direction DD) of each point is calculated using (1) and projected onto a stereonet. (Nx, Ny and Nz are the vector components of the unit normal vector).

$$Oritentation\ for\ stereonet = \begin{cases} DA = cos^{-1}(N_z) \\ DD = tan^{-1}(\frac{N_x}{N_y}) \end{cases} = \begin{cases} DA = 180° - DA \\ DD = DD + 180° \end{cases}, \ for\ DA > 90° \quad (1)$$

- Kernel Density Estimation (KDE) is applied to analyse the orientation data. This technique estimates the probability density function of the orientations, thereby creating a continuous distribution. The resulting density values are visualised as a contour map on the stereonet.
- Using the generated contour map, the discontinuity sets are identified. The major discontinuity sets correspond to regions of local maxima. By applying a user-defined threshold for the maximum number of sets, poles corresponding to these maxima are identified, with a minimum separation cone of 30° between them. Additionally, the user has the option to manually adjust the poles in cases where the automatic identification may be inaccurate due to regional variations.
- The identified maxima poles represent the number of discontinuity sets present in the stope point cloud, and each discontinuity set consists of all points within a 30° cone from its corresponding pole.
- To further refine the results, DBSCAN is applied to the points within each discontinuity set to group them into clusters. The clusters with fewer than 100 points are removed since they do not represent significant discontinuities.

Validation: Significant structures were manually identified and handpicked from the point cloud to validate the results from automatic structural discontinuity mapping. Visible planes were identified in the point cloud, and planar facets were manually fitted to the planes using the Cloud Compare virtual compass tool [9], a commonly used method by geotechnical engineers, to identify the orientations of the prominent discontinuities. These orientations have been used to create a stereonet for the manually picked structures, allowing for a comparison with the automatic structure mapping results and validating the accuracy of the identified discontinuity sets.

III. Results and Discussions

The Hovermap UAV laser scanner was flown for approximately 5 minutes at a constant speed of 1 m/s inside the selected stope used in this study. The raw data is then mutually coregistered using SLAM to form the point cloud file (.las). A cross-section of the resultant point cloud can be seen in (Fig. 2) along with the trajectory taken by the UAV laser scanning system. The stope section of the point cloud consists of approximately 4 million points.

Mean point spacing (PS) and point density (PD) are two important metrics for analysing the quality of a scanned point cloud. Point spacing is the average distance between two adjacent points in a point cloud, whereas point density is the number of points within a given area. The two are directly related, with lower point spacing resulting in higher density, as

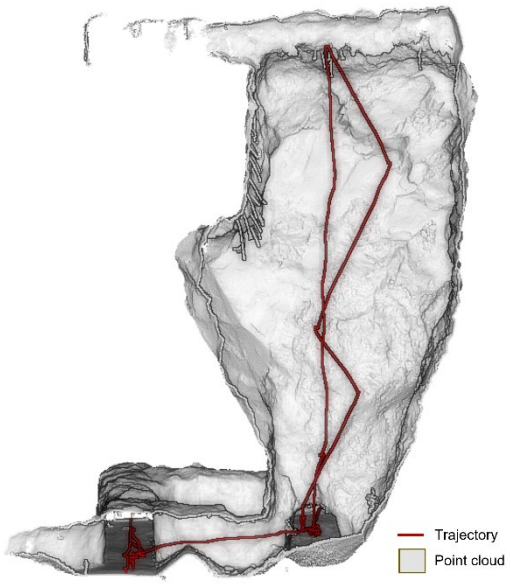

Fig. 2. Cross section of the acquired point cloud showing the trajectory of the UAV laser scanner

can be seen in (2). Point spacing is calculated using triangulation of the entire point cloud. The mean point spacing for the resultant stope point cloud is ~2.5 cm, and point density is ~1600 points/m^2, suggesting a high-resolution point cloud reconstruction.

$$PD = 1/PS^2 \quad (2)$$

After downsampling the point cloud using the voxel grid method with a voxel size of 10cm, the resultant cloud has approximately 700,000 points, which is ~17.5% the size of the original point cloud. The point mean spacing for the downsampled point cloud is ~6.5 cm with a point density of ~240 points/m^2. The downsampling method strategically reduces the number of points so that the processing times can be brought down without compromising the discontinuity mapping process by losing structural information.

The structure mapping algorithm DSE was used to automatically map the discontinuity sets on the down-sampled point cloud. This test was performed on MATLAB R2023a running in a 64-bit Windows system with Intel(R) Xeon(R) W-2245 CPU @ 3.90GHz and 128 GB RAM. The process took a total of 873 seconds from start to end to process the downsampled point cloud. Fig. 3 shows detailed step-by-step results and validation for the discontinuity mapping method.

The stereonet (Fig. 3(a)) displays the orientation of all points in the point cloud, while the contour map in (Fig. 3(b)) highlights the orientation distribution, where the identified maxima poles determine the number of discontinuity sets. A total of 6 discontinuity sets were identified in our test stope and each set is mapped on the stereonet (Fig. 3(c)) as well as colourised in the point cloud for visualisation (Fig. 3(d)).

For validation, visible structures have been handpicked in the point cloud using the Cloud Compare virtual compass tool, and their orientations have been plotted on the stereonet (Fig. 3(e)). When overlaid with the automatically mapped

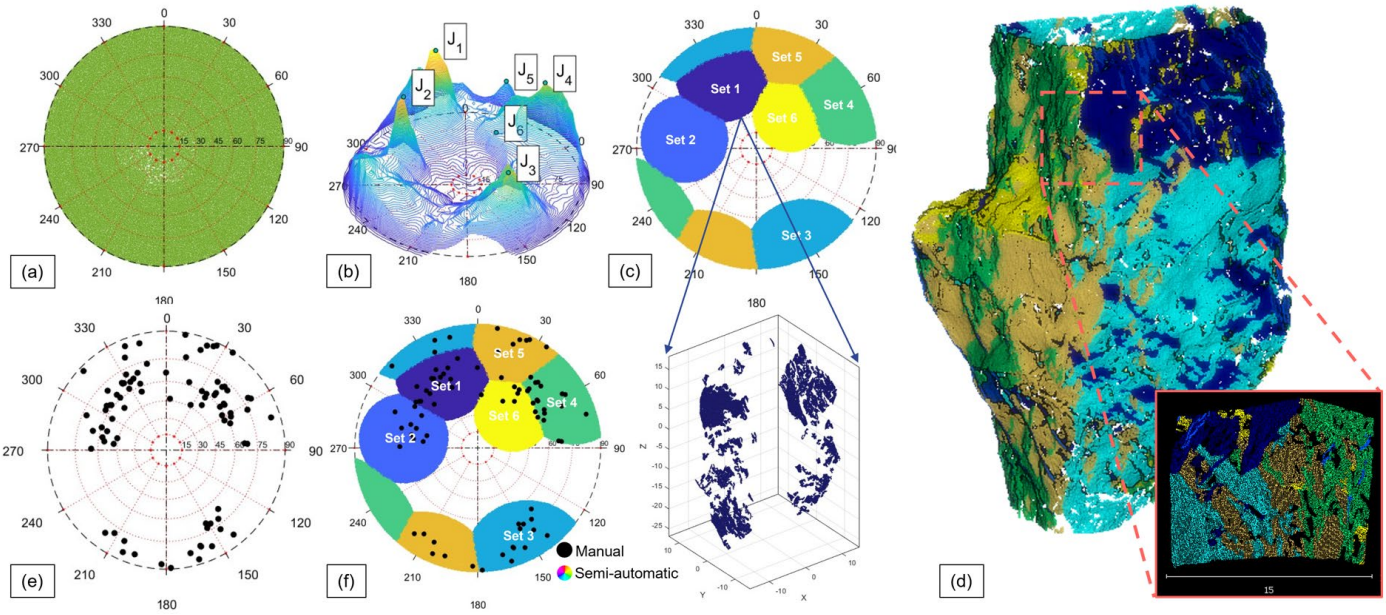

Fig. 3. (a) Stereonet plot of ~700,000 point orientations; (b) Contour map of orientations showing the identified maximas; (c) Discontinuity sets identified by DSE with a plot of the points corresponding to discontinuity set 1; (d) Point cloud of the stope showing the discontinuity sets with close up cross-section view; (e) Manually handpicked discontinuities using Cloud Compare virtual compass tool; (f) Stereonet of manually identified discontinuities overlayed on top of automatically identified discontinuity sets

discontinuity sets (Fig. 3(f)), it was observed that all manually identified discontinuity planes fall within the automatically identified sets, confirming the accuracy of the automatic mapping method. The handpicking process is time-consuming and can take several hours to days, depending on the person's geotechnical expertise. This highlights the automatic technique as a more viable, efficient, and accurate solution. Limitations of the current automated approach include the reliance on empirically defined thresholds within the discontinuity set identification workflow. Future improvements will focus on enhancing autonomy by reducing threshold dependence, incorporating filters for insignificant edges and non-planes, and adopting hierarchical clustering strategies to improve the robustness of discontinuity set identification.

IV. Conclusion

The study demonstrated the advantages of using a UAV laser scanning system for mapping structural discontinuities in underground stopes. This method was successfully tested in a real-world stope environment, showcasing its practicality and effectiveness. Through detailed analysis and validation, the automatic structural mapping approach proved to be both efficient and accurate in identifying discontinuity sets within 3D point clouds. The findings demonstrate the proposed method's potential to enhance safety and productivity in underground stope mapping workflows.

References

[1] H. Daghigh, D. D. Tannant, V. Daghigh, D. D. Lichti, and R. Lindenbergh, "A critical review of discontinuity plane extraction from 3D point cloud data of rock mass surfaces," *Computers & Geosciences,* vol. 169, 2022, doi: 10.1016/j.cageo.2022.105241.

[2] S. Kumar Singh, B. Pratap Banerjee, and S. Raval, "A review of laser scanning for geological and geotechnical applications in underground mining," *International Journal of Mining Science and Technology,* vol. 33, no. 2, pp. 133-154, 2023, doi: 10.1016/j.ijmst.2022.09.022.

[3] R. Stephenson and M. Sandy, "Optimising stope design and ground support – a case study," presented at the Proceedings of the Seventh International Symposium on Ground Support in Mining and Underground Construction, 2013.

[4] S. Guan, Z. Zhu, and G. Wang, "A Review on UAV-Based Remote Sensing Technologies for Construction and Civil Applications," *Drones,* vol. 6, no. 5, 2022, doi: 10.3390/drones6050117.

[5] Z. Luo *et al.*, "Detection of Individual Trees in UAV LiDAR Point Clouds Using a Deep Learning Framework Based on Multichannel Representation," *IEEE Transactions on Geoscience and Remote Sensing,* vol. 60, pp. 1-15, 2022, doi: 10.1109/tgrs.2021.3130725.

[6] H. Sier, X. Yu, I. Catalano, J. P. Queralta, Z. Zou, and T. Westerlund, "UAV Tracking with Lidar as a Camera Sensor in GNSS-Denied Environments," presented at the 2023 International Conference on Localization and GNSS (ICL-GNSS), 2023.

[7] E. Jones, J. Sofonia, C. Canales Cardenas, S. Hrabar, and F. Kendoul, "Advances and applications for automated drones in underground mining operations," presented at the Proceedings of the Ninth International Conference on Deep and High Stress Mining, 2019.

[8] A. J. Riquelme, A. Abellán, R. Tomás, and M. Jaboyedoff, "A new approach for semi-automatic rock mass joints recognition from 3D point clouds," *Computers & Geosciences,* vol. 68, pp. 38-52, 2014, doi: 10.1016/j.cageo.2014.03.014.

[9] S. Thiele, L. Grose, and S. Micklethwaite, "Compass: A CloudCompare workflow for digital mapping and structural analysis," in *EGU General Assembly Conference Abstracts*, 2018, pp. 5548.